Integrated metamaterial surface-emitting antenna for beam steering applications

Pablo Ginel-Moreno*, Alejandro Sánchez-Postigo*, José de-Oliva-Rubio*, Abdelfettah Hadij-ElHouati*,
Winnie N.Ye†, J. Gonzalo Wangüemert-Pérez*, Íñigo Molina-Fernández*, Jens H. Schmid‡,
Pavel Cheben‡ and Alejandro Ortega-Moñux*
*Instituto de Telecomunicación (TELMA), Universidad de Málaga, CEI Andalucía TECH,
E.T.S.I de Telecomunicación, 29010 Malaga, Spain
†Department of Electronics, Carleton University, 1125 Colonel by Drive, Ottawa, Canada
‡National Research Council Canada, Ottawa, K1A 0R6, Canada

***Abstract*—Integrated optical antennas are relevant devices for the development of next-generation LIDAR systems. Here we experimentally demonstrate a new topology to implement long antennas in silicon-on-insulator platform. The designed 2-millimeter-long antenna presents a measured far-field beam divergence of 0.1° and a wavelength sensitivity of 0.13°/nm.**

I. Introduction

Emerging applications such as light detection and ranging (LIDAR) require real-time precise shaping and steering of free-space optical beams [1], [2]. One of the solutions that is gaining more weight in recent years is the integration of optical antennas on silicon chips, through the development of so-called optical phased arrays (OPAs) [3]–[7], which provide rapid steerable beams and high directionality without the need for microelectromechanical systems (MEMS).

Silicon on insulator (SOI) is one of the most widely used platforms for photonic integration due to the high integration it provides as well as its low mass fabrication cost. There are a substantial number of applications that use SOI devices such as optical communications, quantum signal processing, biochemical sensing and even LIDAR systems [8]. However, currently on this platform most optical antennas used to form OPAs follow the same topology based on modulating the lateral roughness of a waveguide. This simple solution works, but it is not optimal for achieving very weak radiation antennas, since the lateral perturbations must be extremely small, in the order of 10 nm [5], [7], making these designs difficult to fabricate with a high precision.

In this talk, we show the experimental demonstration of a 2-millimeter-long, single-etched metamaterial surface-emitting antenna on a 220-nm silicon thick SOI substrate, which presents a measured far-field beam divergence with a full width at half maximum (FWHM) as low as 0.1° and a wavelength sensitivity of 0.13°/nm. The antenna is designed with a minimum feature size (MFS) of 80 nm, which is compatible with deep-UV lithography processes [9].

II. Surface-emitting antenna implementation

The geometry of the antenna is shown in Fig. 1. It consists of two different periodic structures: A subwavelength grating core (SWG) with a period Λ_{SWG} and a set of lateral perturbation segments with a period $\Lambda_g = 4\Lambda_{\mathrm{SWG}}$. The evanescent electric field of the Floquet-Bloch mode propagating in z-direction overlaps with the lateral radiating segments that are separated with a gap (g) from the SWG core, radiating the light out the plane of the chip.

This topology offers two main advantages which allow us to design weak, single-etched surface-emitting antennas. First, the SWG waveguide core is used to control the effective index (n_{FB}) and thus the delocalization of the Floquet-Bloch mode, enabling lateral segments to be placed at a distance that is compatible with the MFS. Second, by controlling the gap (g)

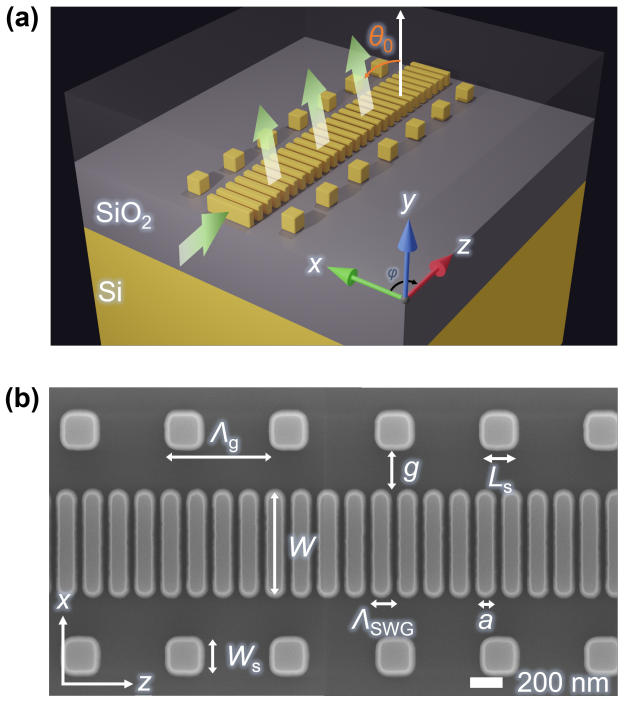

Fig. 1. (a) 3D schematic view of the surface-emitting silicon antenna. (b) SEM image of a fabricated antenna prior to the deposition of the cladding oxide. The emission angle θ_0 is controlled by varying the source wavelength.

it is possible to precisely control the field overlap and hence the radiation strength (α).

Since we are studying a single antenna that is extended in the z-direction several millimeters, it forms a convergent beam in the θ direction (elevation) and a diverging beam in the φ direction (azimuth), with a maximum intensity at $\varphi = 90°$. In Fig. 1 θ_0 denotes the emission angle, which can be controllable with a variation in the wavelength of the light source (λ) as the grating equation says:

$$sin(\theta_0) = n_c sin(\theta_c) = n_{FB} - \frac{\lambda}{\Lambda_g} \quad (1)$$

The antenna is designed using a Floquet-Bloch analysis based on 3D FDTD simulations with periodic boundary conditions [10] for the in-plane (TE) polarization with a silicon thickness $H = 220\,\mathrm{nm}$ and a buried oxide (BOX) layer thickness of $2\,\mu\mathrm{m}$. The details for the selection of the dimensions are specified in our recent publication [11].

III. Experimental results

To characterize experimentally the antenna we used an Agilent 81600B tunable laser as a light source. TE-polarized light with an extinction ratio $> 25\,\mathrm{dB}$ around the band of operation ($1500 - 1620\,\mathrm{nm}$) was coupled from a lensed fiber into the chip through a broadband high-efficiency metamaterial fiber-chip coupler [12]. In addition, we have used two different lens systems, both using an infrared camera. The lens system is responsible for displaying the far field diffracted by the antenna on the sensor plane of the infrared camera. In the first setup an achromatic lens of focal length $f = 35\,\mathrm{mm}$ is used, with which the far-field patterns in Fig. 2(a) have been obtained. From this measurements we can estimate that the wavelength sensitivity of the antenna is 0.13°/nm. On the other hand, in a second setup we used two lenses with focal lengths $f_1 = 100\,\mathrm{mm}$ and $f_2 = 25.4\,\mathrm{mm}$, to achieve a magnification of x5 compared to the first setup. In this way we can estimate the FWHM accurately, obtaining a far-field beam divergence of $0.1°$ (see Fig. 2(b)).

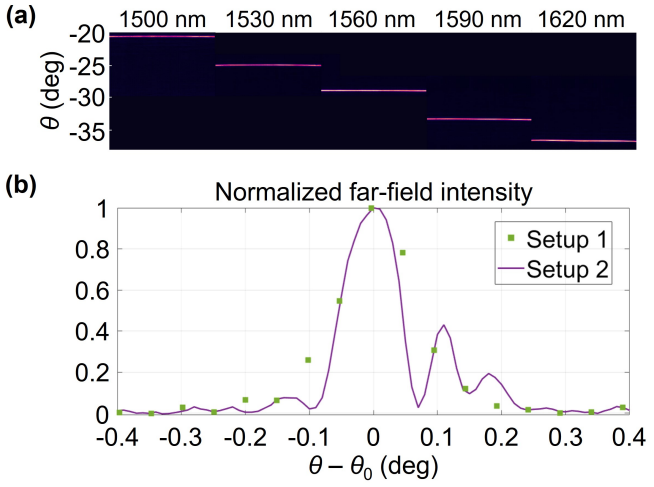

Fig. 2. (a) Far-field intensity measured with the infrared camera and a Fourier-lens system in the range of 1500-1620 nm. (b) Far-field cut at $\varphi = 90°$ for both lens setups. The θ axis is centered at the emission angle ($\theta_0 = -26.6°$) at $1550\,\mathrm{nm}$ wavelength.

IV. Conclusion

We have experimentally demonstrated a new optimized grating topology for silicon-based long surface-emitting antennas that are suitable for applications in one-dimensional (1D) OPAs. We report a measured far-field beam divergence of $0.1°$ in the θ direction, and a scan range of $16°$ with a wavelength variation of $120\,\mathrm{nm}$ (0.13°/nm).

Acknowledgment

HTSN Challenge Program at the NRC of Canada; Universidad de Málaga; Junta de Andalucía (P18-RT-1453, P18-RT-793, UMA18-FEDERJA-219); Ministerio de Ciencia, Innovación y Universidades (FPU16/03401, PID2019-106747RB-I00).

References

[1] M. J. Heck, "Highly integrated optical phased arrays: photonic integrated circuits for optical beam shaping and beam steering," *Nanophotonics*, vol. 6, no. 1, pp. 93–107, 2017.

[2] J. He, T. Dong, and Y. Xu, "Review of photonic integrated optical phased arrays for space optical communication," *IEEE Access*, vol. 8, pp. 188 284–188 298, 2020.

[3] J. K. Doylend, M. J. R. Heck, J. T. Bovington, J. D. Peters, L. A. Coldren, and J. E. Bowers, "Two-dimensional free-space beam steering with an optical phased array on silicon-on-insulator," *Optics Express*, vol. 19, no. 22, p. 21595, 2011.

[4] D. N. Hutchison, J. Sun, J. K. Doylend, R. Kumar, J. Heck, W. Kim *et al.*, "High-resolution aliasing-free optical beam steering," *Optica*, vol. 3, no. 8, p. 887, 2016.

[5] T. Kim, P. Bhargava, C. V. Poulton, J. Notaros, A. Yaacobi, E. Timurdogan *et al.*, "A single-chip optical phased array in a wafer-scale silicon Photonics/CMOS 3D-integration platform," *IEEE Journal of Solid-State Circuits*, vol. 54, no. 11, pp. 3061–3074, 2019.

[6] C. V. Poulton, A. Yaacobi, D. B. Cole, M. J. Byrd, M. Raval, D. Vermeulen *et al.*, "Coherent solid-state LIDAR with silicon photonic optical phased arrays," *Optics Letters*, vol. 42, no. 20, p. 4091, 2017.

[7] S. A. Miller, Y.-C. Chang, C. T. Phare, M. C. Shin, M. Zadka, S. P. Roberts *et al.*, "Large-scale optical phased array using a low-power multi-pass silicon photonic platform," *Optica*, vol. 7, no. 1, p. 3, 2020.

[8] L. Vivien and L. Pavesi, *Handbook of Silicon Photonics*, L. Vivien and L. Pavesi, Eds. Boca Raton: CRC Press, 2013.

[9] E. Luan, V. Donzella, K. Cheung, and L. Chrostowski, "Advances in silicon photonic sensors using sub-wavelength gratings," in *24th OptoElectronics and Communications Conference (OECC) and 2019 International Conference on Photonics in Switching and Computing (PSC)*, vol. 1, 2019.

[10] A. Hadij-ElHouati, P. Cheben, A. Ortega-Moñux, J. G. Wangüemert-Pérez, R. Halir, J. H. Schmid *et al.*, "Distributed Bragg deflector coupler for on-chip shaping of optical beams," *Optics Express*, vol. 27, no. 23, p. 33180, 2019.

[11] P. Ginel-Moreno, A. Sánchez-Postigo, J. De-Oliva-Rubio, A. Hadij-ElHouati, W. N. Ye, J. G. Wangüemert-Pérez *et al.*, "Millimeter-long metamaterial surface-emitting antenna in the silicon photonics platform," *Optics Letters, Vol. 46, Issue 15, pp. 3733-3736*, vol. 46, no. 15, pp. 3733–3736, 2021.

[12] P. Cheben, J. H. Schmid, S. Wang, D.-X. Xu, M. Vachon, S. Janz *et al.*, "Broadband polarization independent nanophotonic coupler for silicon waveguides with ultra-high efficiency," *Optics Express*, vol. 23, no. 17, p. 22553, 2015.